Optimal heterogeneity of a highly renewable pan-European electricity system

Emil H. Eriksen[a], Martin Greiner[b,c]

[a]*Department of Physics and Astronomy, Aarhus University, 8000 Aarhus C, Denmark*
[b]*Department of Mathematics, Aarhus University, 8000 Aarhus C, Denmark*
[c]*Department of Engineering, Aarhus University, 8200 Aarhus, Denmark*

Abstract

The resource quality and the temporal production pattern of variable renewable energy sources varies significantly across Europe. A homogeneous distribution of wind and solar capacities makes inefficient use of the resources, resulting in high system costs. A heterogeneous redistribution of renewable assets maximising the overall capacity factor results in smaller investments in renewable capacities, but higher costs of transmission. An adaptive gradient descent algorithm is used to find optimal distributions of production capacities minimising backup, transmission and renewable capacity costs simultaneously, resulting in lower costs of electricity.

Keywords: renewable energy system, levelised cost of electricity, wind power generation, solar power generation

1. Introduction

The ambitious renewable targets set by the European leaders [1] imply that the renewable penetration will increase significantly in the years to come. Electrification of transportation and other sectors will play a major role in the transition [2, 3].

At present, the leading renewable technologies are wind, solar PV and hydro, of which only wind and solar PV have potential for large-scale expansion. For this reason, the analysis will consider only wind and solar PV explicitly. Since wind and solar PV are both variable renewable energy resources (VRES), backup generation is needed if power outages are to be avoided. Backup generation equals additional system cost and must thus be kept at a minimum.

The backup requirements depend on the mismatch between load and VRES generation. Using the degrees of freedom associated with the choice of VRES assignments, it is possible to shape the temporal pattern towards the load pattern so that the mismatch, and thus the backup requirements, is lowered. Assuming a homogeneous mix between wind and solar across all countries, and that all countries install enough VRES capacities to cover their load on average, only a single degree of freedom remains. This approach is demonstrated e.g. in [4, 5] where balancing and storage optimal wind/solar mixes are found.

Further reductions in backup requirements are possible by exchanging energy between the countries through a transmission network [6, 7]. Other relevant papers on the advantages and costs of grid extensions are [8, 9].

In a conventional energy system, the siting of production capacities is not a concern. No geographical areas are preferable, so the power plants are simply put where the demand is present. For VRES, the situation is more complicated. The primary reason is the geographical variation of the VRES quality. The resource quality is quantified through the capacity factor ν defined as

$$\nu = \frac{\text{Average production}}{\text{Rated capacity}}. \quad (1)$$

The capacity factor is a number between 0 and 1, where 0 means no production and 1 means maximum production at all times. Capacity factors for the European countries for onshore wind, offshore wind and solar PV are listed in table 1. The capacity factors were calculated using the Renewable Energy Atlas [10] (REA). The VRES layout at country level was chosen as a homogeneous distribution across the 50% best sites. For wind conversion, the power curve of the Vestas V90 3.0MW turbine was assumed. For solar conversion, the Scheuten P6-54 solar PV panel oriented south and tiled from horizontal to a degree equal to the latitude of installation was applied.

The second reason is the geographical variation of the temporal production pattern of each VRES. This effect is particularly important for wind since Europe is large compared to the wind correlation length of $\approx$ 1000 km [11]. Allocating resources taking this effect into account, it is possible to smooth out the aggregated temporal pattern, or even shape it towards the temporal pattern of the load as done by [4, 5] with the wind/solar mix.

With these points in mind, allocating resources proportional to the mean load of a country in accordance with a homogeneous wind/solar mixing factor does not seem ideal. In this paper, the homogeneous assumption

---

Email addresses: `emilhe@phys.au.dk` (Emil H. Eriksen), `greiner@eng.au.dk` (Martin Greiner)

is lifted. Different approaches to cope with the resulting large number of degrees of freedom are considered ranging from heuristic layouts constructed from resource quality knowledge to layouts obtained through numerical optimization. The objective is to find heterogeneous layouts with properties superior to the homogeneous layouts, in particular a lower cost of electricity.

This paper is organised as follows: Section 2 discusses the general modelling of the electricity system, the key metrics and the construction of heterogeneous layouts. In section 3 the performance of the different layouts and the resulting renewable penetrations for individual European countries are discussed. Section 4 contains an analysis of the sensitivity of the results to reductions in solar costs and to expansions in offshore wind capacities. We conclude the paper with a discussion on the results and an outlook on future research.

2. Methods

2.1. The electricity network

The European electricity network is modelled using a 30-node model where each node represents a country. The nodal load is determined from historical data, while wind and solar production data are calculated using a combination of weather data and physical models[10]. Initially, wind is assumed to be onshore only. For each node n the generation from VRES,

$$G_n^R(t) = G_n^W + G_n^S, \tag{2}$$

can be expressed through two parameters. The penetration γ determines the amount of energy generated relative to the mean load of the node,

$$\langle G_n^R \rangle = \gamma_n \langle L_n \rangle, \tag{3}$$

while the mixing parameter α fixes the ratio between wind and solar,

$$\langle G^W \rangle = \langle G_n^R \rangle \alpha_n, \tag{4}$$

$$\langle G^S \rangle = \langle G_n^R \rangle (1 - \alpha_n). \tag{5}$$

The nodal difference between VRES generation and load

$$\Delta_n(t) = G_n^R(t) - L_n(t) \tag{6}$$

is called the mismatch. To avoid power outages, the demand must be matched at all times. Since storage is not considered, any power deficits must be covered by backup generation. Dispatchable resources are not modelled explicitly, but are considered a part of the backup generation. If $\Delta_n(t) \geq 0$, excess energy can be curtailed $C_n(t)$, while if $\Delta_n(t) < 0$ backup generation $G_n^B(t)$ is needed.

$$C_n(t) = +\max(\Delta_n(t), 0) \tag{7}$$

$$G_n^B(t) = -\min(\Delta_n(t), 0) \tag{8}$$

Summing the two terms, we get the nodal balancing $B_n(t) = C_n(t) + G_n^B(t)$. It is possible to lower the balancing needs by transmission. Nodes with excess production export energy $E_n(t)$, allowing nodes with an energy deficit to import energy $I_n(t)$ to (partly) cover their energy deficit. The nodal injection, $E_n(t) - I_n(t)$, is denoted $P_n(t)$. This leads to the nodal balancing equation,

$$G_n^R(t) - L_n(t) = B_n(t) + P_n(t). \tag{9}$$

The vector of nodal injections $\mathbf{P}$ is called the injection pattern. The actual imports and exports, and thus the injection pattern, depend on the business rules of the nodal interactions. It is convenient to express business rules in terms of a two step optimization problem. The top priority is to minimize the backup generation,

$$\text{Step 1:} \quad \min_{\mathbf{P}} \quad \sum_n G_n^B = G_{min}^B \tag{10}$$
$$\text{s.t.} \quad f_l^- \leq f_l \leq f_l^+$$

where $f_l^\pm$ denote any flow constraints on the network. The minimal backup energy can be realized by a number of injection patterns. The degeneracy is removed by choosing the injection pattern that minimizes the sum of squared flows,

$$\text{Step 2:} \quad \min_{\mathbf{P}} \quad \sum_l f_l^2$$
$$\text{s.t.} \quad f_l^- \leq f_l \leq f_l^+ \tag{11}$$
$$\text{s.t.} \quad \sum_n G_n^B = G_{min}^B.$$

The purpose of the second minimization step is twofold. First, it ensures that the nodes exchange energy in the most localized way. Secondly, it guarantees that the solution resembles a physical flow[12].

2.2. Key metrics

Inspired by [13], the energy system cost is calculated based on a few key parameters. Besides the cost of the VRES capacities, $\mathcal{K}^{\mathcal{W}}$ and $\mathcal{K}^{\mathcal{S}}$, costs for the backup system and the transmission network are included. The backup system cost is split into two components, the cost of backup capacity $\mathcal{K}^B$ (including maintance) and the cost of backup energy E^B. The backup capacity cost covers expenses related to keeping the power plants online while the backup energy cost accounts for the actual fuel cost. Expressed in units of the average yearly load, the backup energy is given by

$$E^B = \frac{\sum_n \sum_t G_n^B(t)}{\sum_n \sum_t L_n(t)} = \sum_n \frac{\langle G_n^B \rangle}{\langle L_n \rangle}. \tag{12}$$

In principle, the backup capacity is fixed by a single extreme event. However with this definition, the results will be highly coupled to the particular data set used. To

decrease the coupling, the 99% quantile is used rather than the maximum value,

$$q_n = \int_0^{K_n^B} p_n(B_n) dB_n \qquad (13)$$

where $p_n(B_n)$ is the time sampled distribution of backup power and $q_n = 0.99$. With this choice, the backup system will be able to cover the demand 99% of the time. The remaining 1% is assumed to be cover by unmodeled system components like storages or demand side management. In accordance, the transmission capacity $\mathcal{K}^T$ is defined so that the demand is met 99% of the time. Since transmission can be positive and negative, the larger of the absolute value of the 0.5% and the 99.5% quantile is used rather than the 99% quantile,

$$\mathcal{K}^T = \sum_l \mathcal{K}_l^T \qquad (14)$$

with

$$\mathcal{K}_l^T = \max\{-Q_{0.5\%}, Q_{99\%}\} \qquad (15)$$

and

$$x = \int_{-\infty}^{Q_x} p_n(f_l) dF_l. \qquad (16)$$

Cost assumptions for the elements of an energy system vary greatly across the literature [13]. In this study, the cost assumption published by [14] have been adapted, see table 2. The cost assumptions are in the low end for VRES which reflects the expectation that the cost of VRES will go down in the future as the penetration increases [15].

Table 2: Cost assumptions for different assets.

Asset	CapEx [/W]	Fixed OpEx [/kW/y]	Variable OpEx [/MWh]
CCGT	0.9	4.5	56.0
Solar PV	1.5	8.5	0.0
Offshore wind	2.0	55.0	0.0
Onshore wind	1.0	15.0	0.0

From the VRES penetration, the mixing factor and the mean load, the effective production of each node can be calculated. Dividing by the associated capacity factor, one arrives at the capacity. Except for transmission capacity, the present value of each element can be calculated directly as

$$V = \text{CapEx} + \sum_t \frac{\text{OpEx}_t}{(1+r)^t} \qquad (17)$$

where r is the return rate assumed to be 4%. The transmission capacity cannot be translated directly into cost as the cost depends on the length and the type of the link. Link lengths have been estimated as the distance between the country capitals. Link costs are assumed to be 400€ per km for AC links and 1,500€ per km for HVDC links. For HVDC links, an additional cost of 150,000€ per converter station (one in each end) is added [8, 9, 16]. The layout of AC and DC links has been constructed by [6] from ENTSO-E data.

Given the element costs, the system cost V_{sys} is calculated by summation. To allow for comparison of different energy systems, the levelised cost of electricity (LCOE) is a convenient measure. The LCOE is the cost that every unit of energy produced during the lifetime of the project must have to match the present value of investment [17],

$$\text{LCOE} = \frac{V_{sys}}{\sum_t \frac{L_{EU,t}}{(1+r)^t}}. \qquad (18)$$

See [13] for more details on the cost calculation.

2.3. Heuristic layouts

The simplest way to distribute the renewable resources would be to assign the resources homogeneously (relative to the mean load of the node) so that $\gamma_n = \gamma$ (and $\alpha_n = \alpha$). However this assignment might not be ideal since the capacity factors vary significantly between the nodes. Having this point in mind, an intuitive way to proceed would be to assign resources proportional to the resource quality. To generalise the idea, the resource quality expressed through ν is raised to an exponent β as suggested by [14]. For a wind only layout, the γ values are given by

$$\gamma_n^W = \left(\nu_n^W\right)^\beta \frac{\langle L_{EU} \rangle}{\sum_m \langle L_m \rangle \left(\nu_m^W\right)^\beta}. \qquad (19)$$

An equivalent expression for the solar only layout is obtained by the substitution $W \to S$. Examples for $\beta = 1$ are shown in figure 1. In the layout illustrations, each bar represents a country n. The height of the bar is γ_n while the mix α_n between onshore wind (dark blue) and solar (yellow) is expressed through the bar colouring. β layouts for any value of α can be expressed as a linear combination of the wind and solar only layouts with

$$\gamma_n = \alpha \gamma_n^W + (1-\alpha)\gamma_n^S \qquad (20)$$

and

$$\alpha_n = \frac{\alpha \gamma_n^W}{\alpha \gamma_n^W + (1-\alpha)\gamma_n^S}. \qquad (21)$$

For practical reasons, it is not possible to realise arbitrarily heterogeneous layouts. To constrain heterogeneity, the heterogeneity factor K is introduced by requiring

$$\frac{1}{\text{K}} \leq \gamma_n \leq \text{K}. \qquad (22)$$

With this definition, K = 1 corresponds to a homogeneous layout (in terms of γ) while K = ∞ represents unconstrained heterogeneity.

Although the capacity factor of a β layout is higher than the capacity factor of the homogeneous layout (for $\beta > 0$), it is possible to achieve an even higher capacity factor without violating the constraints in equation (22). In the wind/solar PV only cases, the capacity factor is maximised by assigning $\gamma_n = K$ to the countries with the highest capacity factor for wind/solar PV and $\gamma_n = \frac{1}{K}$ to the remaining countries, except for a single in-between country. Examples for K = 2 are shown in figure 1. Similar to the β layouts, ν_{max} layouts for arbitrary α values can be expressed as a linear combination of the wind and solar PV only layouts.

2.4. Optimized layouts

The optimization objective is minimization of the LCOE with respect to the 60 variables $\gamma_1, ..., \gamma_N, \alpha_1, ..., \alpha_N$. A number of optimization algorithms were tested of which adaptive gradient descent(AGD),was found to most effective. All optimized layouts have been obtained using an AGD algorithm. They will be denoted AGD layouts.

3. Results

An overview of the key variables is shown in figure 2. For backup energy and backup capacity, the optimal α value is around 0.9, which is slightly higher than the values found by [4, 5]. The difference can be attributed to the different data sets used for wind and solar PV. For transmission capacity, the minimum is around $\alpha = 0.4$, indicating a high share of solar PV. While the wind correlation length is around ≈ 1000 km [11] and thus smaller than Europe, the occurrence of sun light is highly correlated for the European countries. Therefore, a high wind share causes more power to flow between the countries.

The main variable of interest, the LCOE, shows a very clear tendency. The more wind, the lower the cost. The tendency is a consequence of the significantly higher cost of energy production for solar PV compared to onshore wind. The CapEx is 50% higher and the capacity factor, on average, around 40% lower. Even though the cost of backup energy, backup capacity and transmission capacity is lowered by the introduction of a small solar component, the savings do not compensate the higher cost of production for solar PV compared to onshore wind.

The cost components for the optimal β, ν_{max} and AGD layouts are shown in figure 3. From this figure it is clear that the VRES cost is dominating, which explains the wind monopole for the β and ν_{max} layouts. The AGD layouts include a small solar component, decreasing with increasing K values. The AGD layouts are noticeably cheaper than both the β and the ν_{max} layouts, primarily due a decrease in transmission costs.

The optimal β, ν_{max} and AGD layouts are shown in figure 4. Note that for $K = 1$, the β and the ν_{max} layouts are both equal to the homogeneous layout. From figures 4b and 4c we see that the ν_{max} and the AGD layouts are quite similar. These figures also explain why the
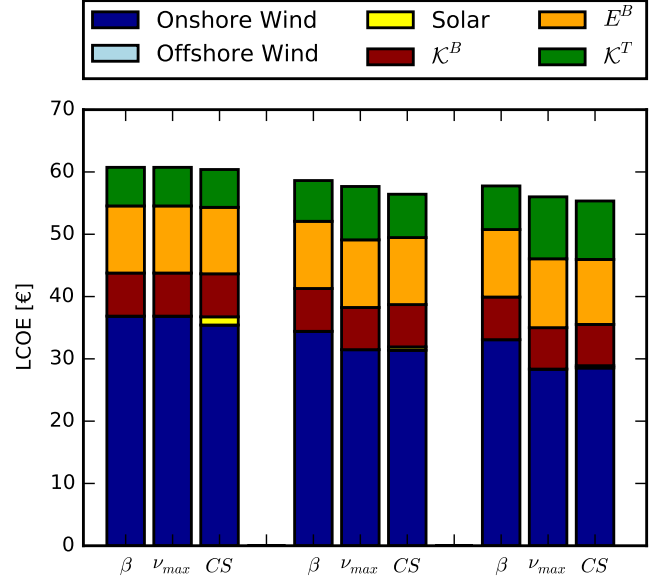

Figure 3: Cost details for the optimal β, ν_{max} and AGD layouts for K = 1 (left), 2 (middle) and 3 (right).

AGD algorithm is able to include a solar component at a competitive cost; unlike the β and ν_{max} layout definitions, the AGD algorithm has the freedom to assign solar only to countries with poor wind resources, e.g. Serbia (RS) and Slovenia (SI). In addition, the AGD algorithms reallocates some of the wind resources, e.g. from Latvia (LV) to Portugal (PT), to counteract power flows as, see figure 5.

4. Sensitivity analysis

4.1. Reduced solar cost

For the β as well as the ν_{max} layouts, the optimal α values are 1. Even for the AGD layouts, only a minor solar component is present. As mentioned previously, this tendency is a consequence of the higher cost of energy production for solar PV compared to onshore wind. In this section, the sensitivity of the optimum to the the solar cost is explored. In figure 6, the LCOE as a function of α is shown, similar to the lower left of figure 2, when the solar cost is reduced by a factor of 2 and 4 respectively.

A reduction of the solar cost by a factor of 2 shifts the optimal mix from 1 to around 0.9 similar to the optimum for backup energy and backup capacity. The shift indicates that the energy production cost for solar PV is becoming competitive to onshore wind. At a cost reduction of a factor of 4, the optimal mix is shifted further to around 0.7, indicating that the energy production cost for solar PV is now lower than for onshore wind. The favouring of wind even when the production cost of solar PV is lower is a consequence of the strong diurnal pattern leading to high backup requirements. The exact α values are listed in table 3.

Table 3: Alpha values for optimal layouts for different scalings of the solar cost.

(a) Cost reductions by a factor of 2.

	K = 1	K = 2	K = 3
β	0.87	0.93	0.93
ν_{max}	0.87	0.87	0.87
CS	0.82	0.92	0.93

(b) Cost reductions by a factor of 4.

	K = 1	K = 2	K = 3
β	0.67	0.67	0.67
ν_{max}	0.67	0.67	0.73
CS	0.68	0.78	0.81

4.2. Offshore wind

In the previous discussion, wind was assumed to be onshore only. By January 2014, the total European onshore wind capacity was 120.8GW, while the offshore capacity was 8.0GW [18]. While these numbers confirm the onshore-only assumption to be reasonable at present, the increasing share of offshore wind raises the question how the LCOE will be affected by the introduction of an offshore component. The immediate expectation is a significant increase in the LCOE since the cost of offshore wind is more than 100% higher compared to onshore wind due to foundation expenses along with increased maintenance costs. On the other hand, capacity factors for offshore sites are generally significantly higher than for onshore sites as indicated by table 1.

It would be possible to introduce offshore wind on equal footing with onshore wind and solar PV. However, since offshore wind is much more expensive, an optimized layout would pose a 0% offshore component, which is not a very interesting nor surprising result. Instead, a fixed offshore component is introduced by splitting the wind component into an onshore γ^W and an offshore $\tilde{\gamma}^W$ component,

$$\gamma^W \to \gamma^W + \tilde{\gamma}^W, \qquad (23)$$

for countries with suitable offshore regions. Explicitly these are: Denmark, Germany, Great Britain, Ireland, the Netherlands, France, Belgium, Norway and Sweden. Other countries retain onshore wind only. The magnitude of the offshore component is assigned by requiring that the offshore wind power generation accounts for a fixed share of the total wind power generation,

$$\text{offshore share} = \frac{\tilde{\gamma}^W}{\gamma^W + \tilde{\gamma}^W}. \qquad (24)$$

Cost details for optimized layouts with fixed offshore shares of 0%, 25% and 50% are shown in figure 7.

From figure 7 it is clear that the introduction of an offshore component increases the LCOE. However, the increase in LCOE is not dramatic. While the cost of wind
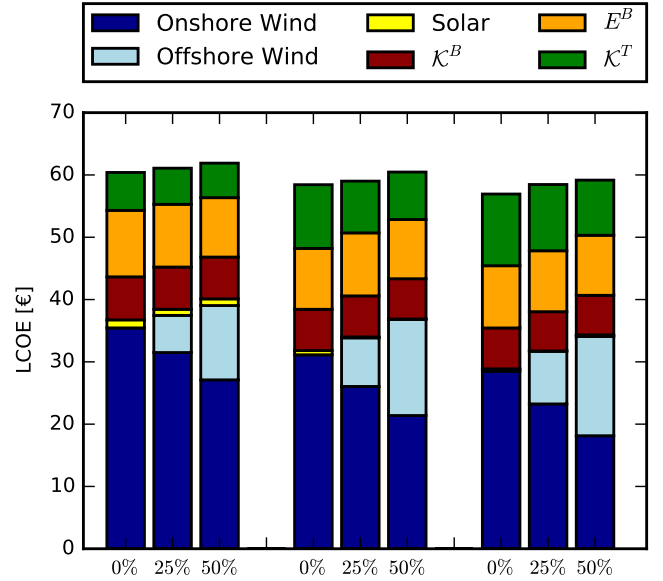

Figure 7: Cost details for the AGD optimal layouts for K = 1 (left), 2 (middle) and 3 (right) for offshore shares of 0%, 25% and 50%.

energy increases significantly, the cost of backup and transmission decreases slightly. The decrease is a consequence of the difference in the temporal production pattern from onshore to offshore wind. In some time steps the onshore production is low while the offshore production is high. The introduction of an offshore component thus tends to smooth out the wind production time series. As a side effect, solar becomes less favourable as illustrated by figure 7. The AGD optimized layouts for an offshore share of 50% are shown in figure 8.

5. Discussion and conclusions

The dependence on the layout of VRES of a number of key parameters along with the resulting LCOE has been investigated. It was found that the backup and transmission costs are significant, but main costs are associated with the VRES capacities. The VRES capacity costs can be lowered by allocating more resources to countries with high capacity factors. At a heterogeneity factor of $K = 2$, meaning that each country installs VRES capacities covering a minimum of 50% and maximum of 200% of their mean load, the LCOE can be lowered by almost 5% by choosing the heuristic ν_{max} layout which maximises the overall capacity factor. Further reduction of the cost can be achieved by reducing backup and/or transmission costs. Using the adaptive gradient descent algorithm, such a layout was found to reduce the LCOE by an additional 2%. While the additional cost reduction of 2% relies heavily on the current network structure, the primary cost reduction is of a more general nature. It can be attributed to the general tendency for the heterogeneous layouts to move wind capacities towards the North Sea countries. Since

the wind resource quality is better than for the central and southern countries, the reallocation results in lower costs.

The cost optimal layouts considered in the main analysis are almost exclusively based on onshore wind. The reason is that onshore wind is significantly cheaper than solar, partly due to lower capital expenses, partly due to higher capacity factor. It was found that the cost of solar must decrease by a factor of ≈ 2 for a significant solar component to become profitable. Besides lowering the capital expenses, the solar cost could also be lowered by increasing the capacity factor. Based on data from [10], the capacity factor can be increased by $\approx 40\%$ by applying dual axis tracking compared to the fixed position installation assumed in table 1.

The main analysis considered onshore wind only, but the effect of introducing an offshore component was also discussed. Foundation expenses and increased maintenance costs makes offshore wind significantly more expensive than onshore wind. Some of the additional expenses are compensated by higher offshore capacity factors along with a more stable temporal production pattern, but at the end of the day, offshore wind is still more expensive than onshore wind. However, there are other incentives for offshore wind. The opposition from residents is usually lower than for onshore wind, and the potential for expansion larger. The number of suitable onshore sites are final, and when they are exhausted, offshore wind might be the best alternative.

In conclusion, it was found that a heterogeneous layout with wind resources shifted towards the North Sea countries decreases the LCOE by around 5% compared to the homogeneous layout at the optimal mix. An additional reduction by 2% was possible by taking also transmission and backup costs into account.

The effect of integrating one or more storage elements in the electricity system has not been considered in this paper. Promising storage projects are already in the making, so by the time Europe reaches $\gamma = 1$, commercial large scale storage systems are presumably available. A natural extension of this paper would be to include various types of storage.

Bibliography

[1] European Commission. A roadmap for moving to a competitive low carbon economy in 2050. Technical report, EC, March 2011.

[2] James H. Williams, Andrew DeBenedictis, Rebecca Ghanadan, Amber Mahone, Jack Moore, William R. Morrow, Snuller Price, and Margaret S. Torn. The Technology Path to Deep Greenhouse Gas Emissions Cuts by 2050: The Pivotal Role of Electricity. Science, 335:53–59, 2012. http://dx.doi.org/10.1126/science.1208365.

[3] McKinsey & Company, KEMA, The Energy Futures Lab at Imperial College London, Oxford Economics, and ECF. Roadmap 2050 – A practical guide to a prosperous, low-carbon Europe. Technical report, European Climate Foundation, http://www.roadmap2050.eu/, April 2010. Online, accessed June 2012.

[4] Heide, D., von Bremen, L., Greiner, M., Hoffmann, C., Speckmann, M., and Bofinger, S. Seasonal optimal mix of wind and solar power in a future, highly renewable Europe. Renewable Energy, 35(11):2483–2489, 2010.

[5] Heide, D., Greiner, M., Von Bremen, L., and Hoffmann, C. Reduced storage and balancing needs in a fully renewable European power system with excess wind and solar power generation. Renewable Energy, 36(9):2515–2523, 2011.

[6] Rolando A. Rodriguez, Sarah Becker, Gorm Bruun Andresen, Dominik Heide, and Martin Greiner. Transmission needs across a fully renewable European power system. Renewable Energy, 63:467–476, March 2014.

[7] Sarah Becker, Rolando A. Rodríguez, Gorm B. Andresen, Stefan Schramm, and Martin Greiner. Transmission grid extensions during the build-up of a fully renewable pan-European electricity supply. Energy, 64:404–418, January 2014.

[8] Schaber, K., Steinke, F., and Hamacher, T. Transmission grid extensions for the integration of variable renewable energies in Europe: Who benefits where? Energy Policy, 43:123 – 135, 2012.

[9] Schaber, K., Steinke, F., Mühlich, P., and Hamacher, T. Parametric study of variable renewable energy integration in Europe: Advantages and costs of transmission grid extensions. Energy Policy, 42:498–508, 2012.

[10] Gorm Bruun Andresen, Anders Aspegren Sndergaard, and Martin Greiner. Validation of danish wind time series from a new global renewable energy atlas for energy system analysis. Elsevier, 2014.

[11] J. Widen. Correlations between large-scale solar and wind power in a future scenario for sweden. IEEE Transactions on Sustainable Energy, 2(2):177–184, 2011.

[12] Magnus Dahl. Power-flow modeling in complex renewable electricity networks. Master's thesis, Aarhus University, 2015.

[13] Rodriguez, R.A., Becker, S., and Greiner, M. Cost-optimal design of a simplified, highly renewable pan-European electricity system. 2014.

[14] Rolando A. Rodriguez. Weather driven power transmission in a highly renewable European electricity network. PhD thesis, Aarhus University, 2014.

[15] Kost, C., Schlegl, T., Thomsen, J., Nold, S., and Mayer, J. Levelized cost of electricity: renewable energies. Technical report, Fraunhofer Institute for solar energy systems ISE, 2012. Online, retrieved October 2013.

[16] McKinsey. RoadMap 2050: A Practical Guide to a Prosperous, Low-Carbon Europe. Technical report, European Climate Foundation, 2010. Online, retrieved October 2013.

[17] W. Short, D. Packey, and T. Holt. A manual for the economic evalua- tion of energy efficiency and renewable energy technologies. Technical report, National Renewable Energy Laboratory, 1995.

[18] G. Corbetta, I. Pineda, and J. Wilkes. Wind in power 2014 european statistics. Technical report, The European Wind Association, 2015.

Table 1: Capacity factors ν_n^w, $\tilde{\nu}_n^w$ and ν_n^s for onshore wind, offshore wind and solar PV for the European countries.

	ν_n^w	$\tilde{\nu}_n^w$	ν_n^s		ν_n^w	$\tilde{\nu}_n^w$	ν_n^s		ν_n^w	$\tilde{\nu}_n^w$	ν_n^s
AT	0.16	-	0.15	DE	0.26	0.53	0.13	NO	0.31	0.44	0.12
BE	0.27	0.49	0.12	GB	0.39	0.53	0.11	PL	0.22	0.42	0.13
BA	0.16	-	0.16	GR	0.17	0.43	0.17	PT	0.23	0.25	0.18
BG	0.14	0.24	0.17	HU	0.14	-	0.15	RO	0.13	0.31	0.16
HR	0.21	0.28	0.16	IE	0.43	0.47	0.10	RS	0.11	-	0.16
CZ	0.19	-	0.14	IT	0.17	0.21	0.17	SK	0.15	-	0.15
DK	0.45	0.54	0.12	LV	0.29	0.42	0.11	SI	0.09	-	0.15
EE	0.33	0.41	0.11	LT	0.25	0.40	0.11	ES	0.19	0.26	0.18
FI	0.23	0.41	0.10	LU	0.24	-	0.13	SE	0.26	0.41	0.12
FR	0.25	0.42	0.15	NL	0.34	0.53	0.12	CH	0.16	-	0.16
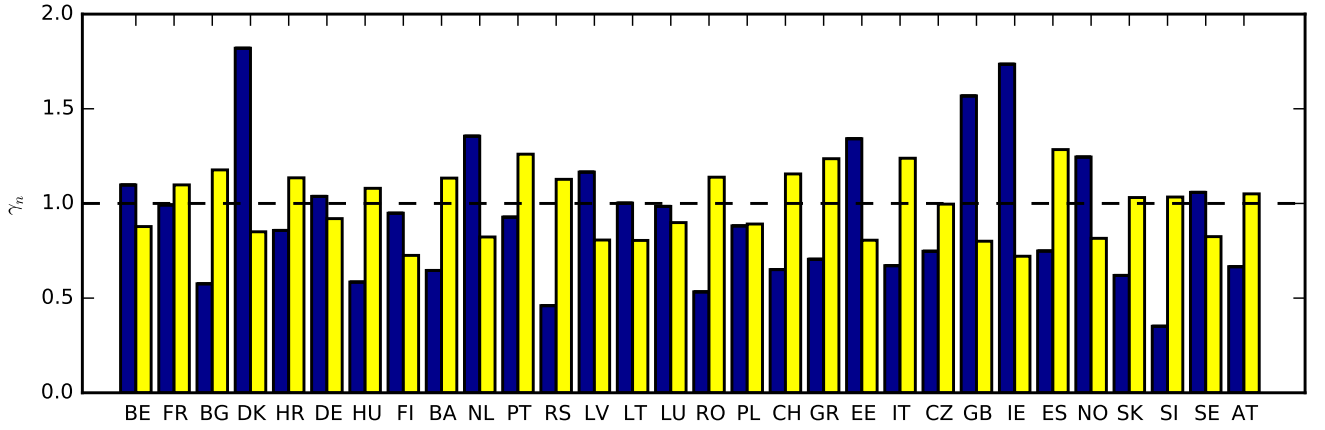
(a) Examples of β layouts for $\beta = 1$.
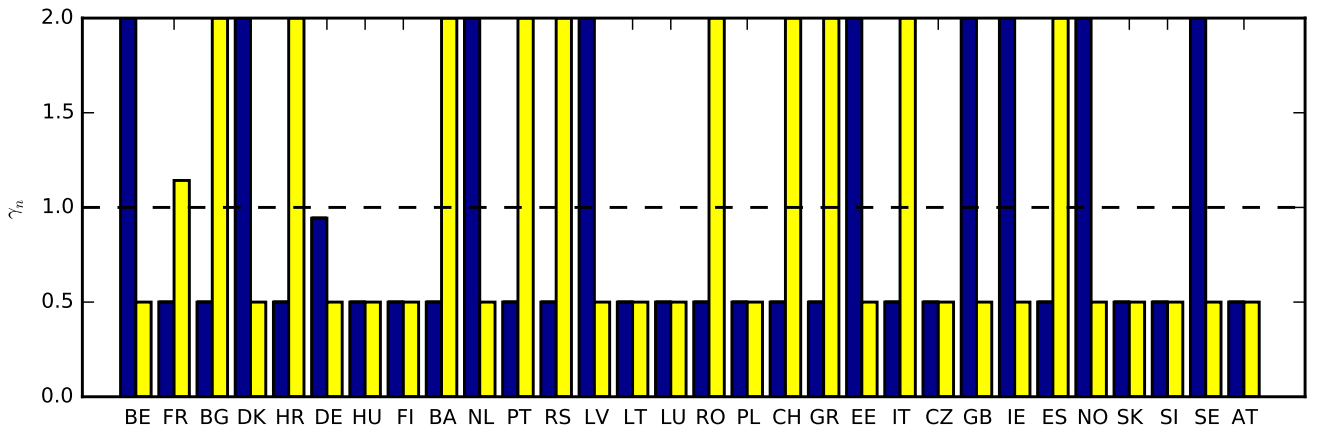
(b) Examples of ν_{max} layouts constrained by K = 2 .

Figure 1: Examples of heuristic layouts. In each sub figure, two sets of bars corresponding to the $\alpha = 1$ and the $\alpha = 0$ layouts respectively are shown.
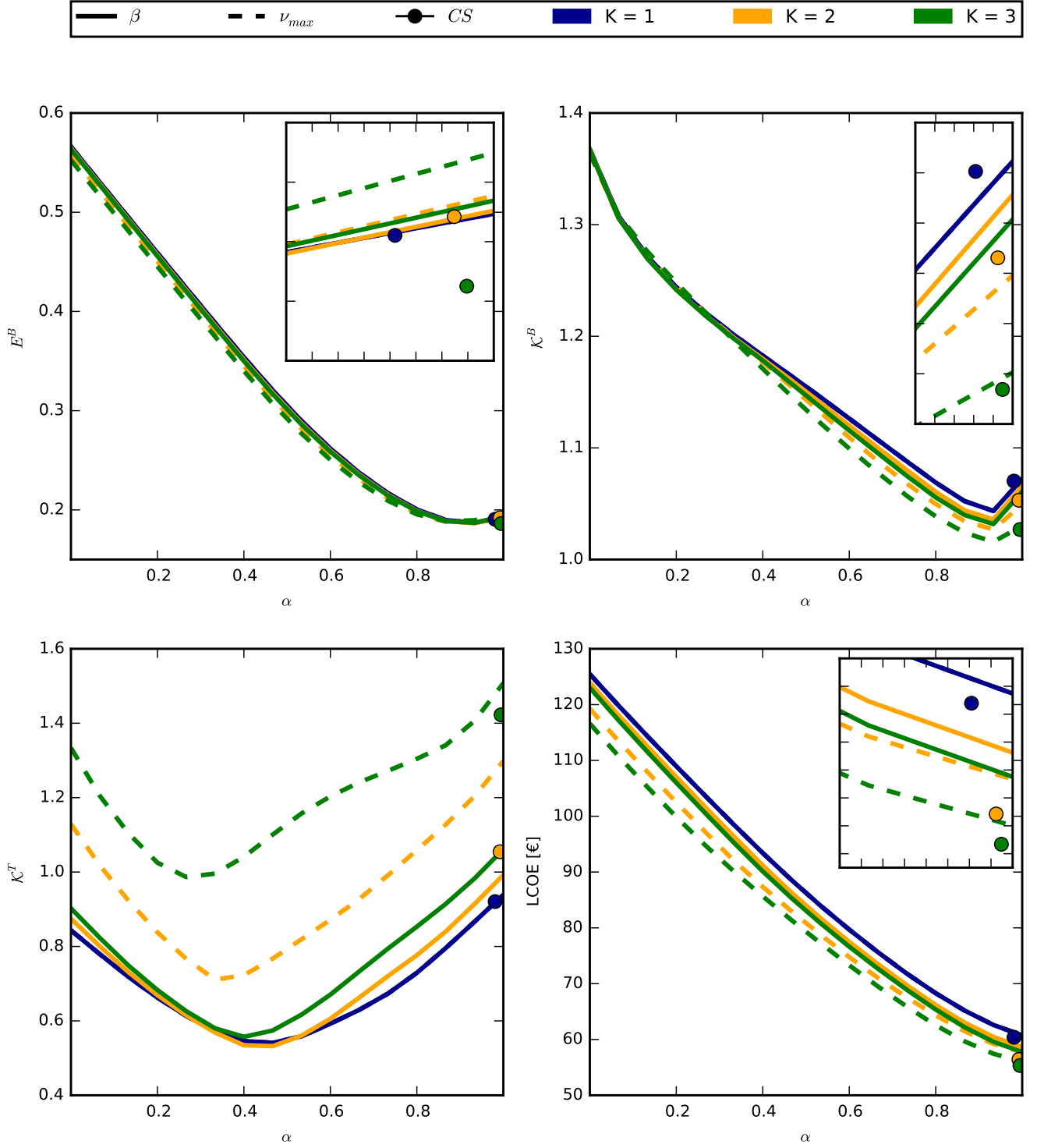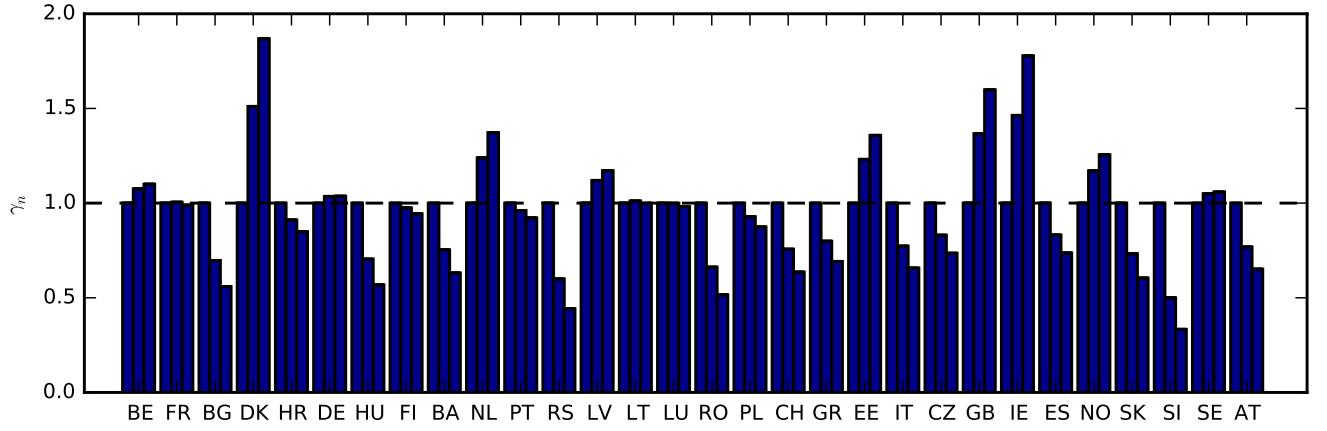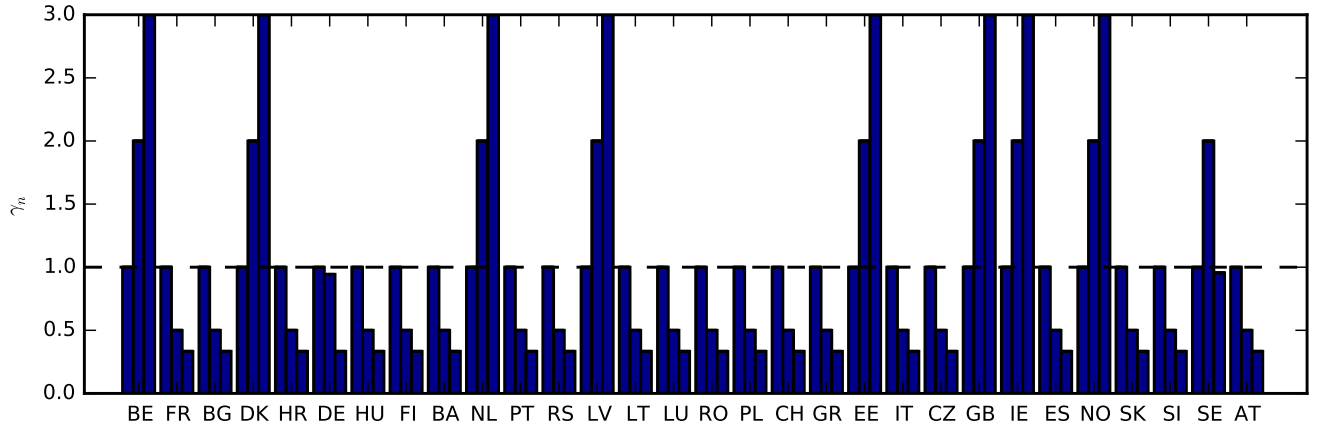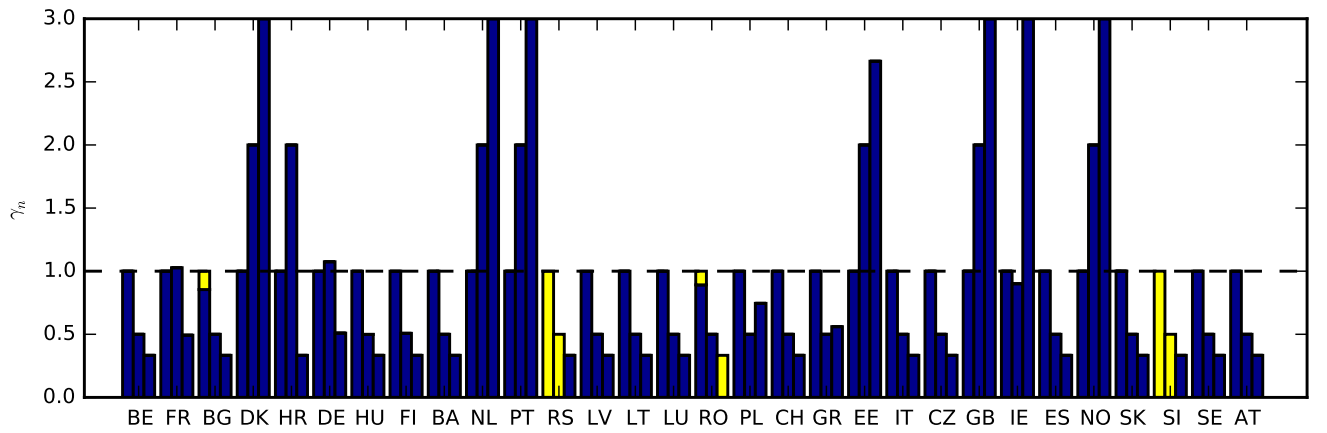
Figure 2: Overview of the key variables, backup energy E^B, backup capacity $\mathcal{K}^B$ and transmission capacity $\mathcal{K}^T$ along with the associated LCOE.

(a) Optimal β layouts (optimal mix at $\alpha = 1$).

(b) Optimal ν_{max} layouts (optimal mix at $\alpha = 1$).

(c) AGD optimized layouts.

Figure 4: Optimal layouts. In each sub figure, three sets of bars corresponding to values of K = 1 (left), 2 (middle), and 3 (right) are shown.

(a) Link usage for the ν_{max} layout constrained by K = 3.

(b) Link usage for the AGD layout constrained by K = 3.

Figure 5: Overview of link usage. AC links are shown in black while HVDC links are shown in red. Link capacities are indicated relative to the highest flow (110 GW between Great Britain and France in figure 5a). In the AGD layout, resources are allocated in a way that tends to decrease the load on especially the HVDC links. This tendency can be attributed to the fact that the cost of HVDC links is significantly higher than the cost of AC links. An exception is Great Britain where ν^W is so high that the resulting low cost of wind energy outweighs the cost of the HVDC connections.
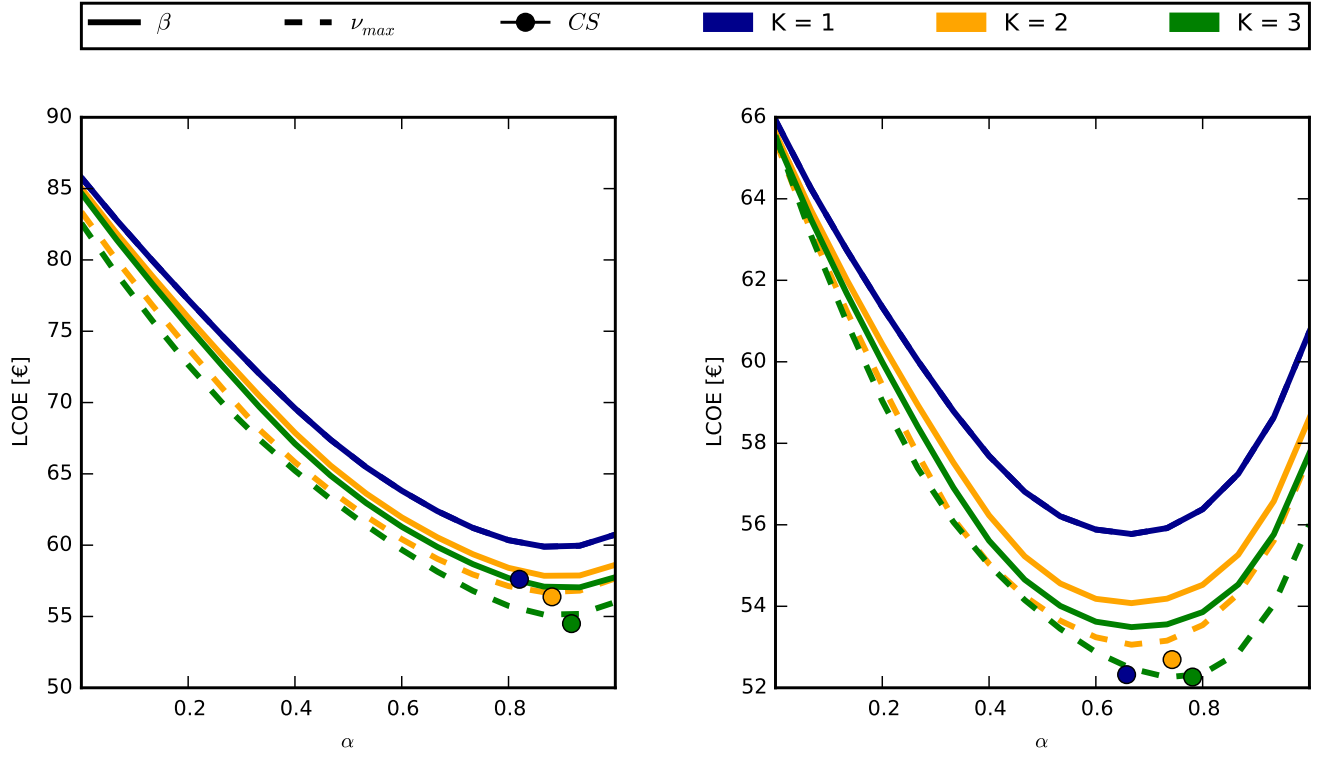
Figure 6: LCOE for different scalings of the solar cost. Shown are cost reductions by a factor of 2 (left) and 4 (right). From the figure, it is clear that for solar PV to be cost competitive to onshore wind, the cost must drop by a factor of ≈ 2.
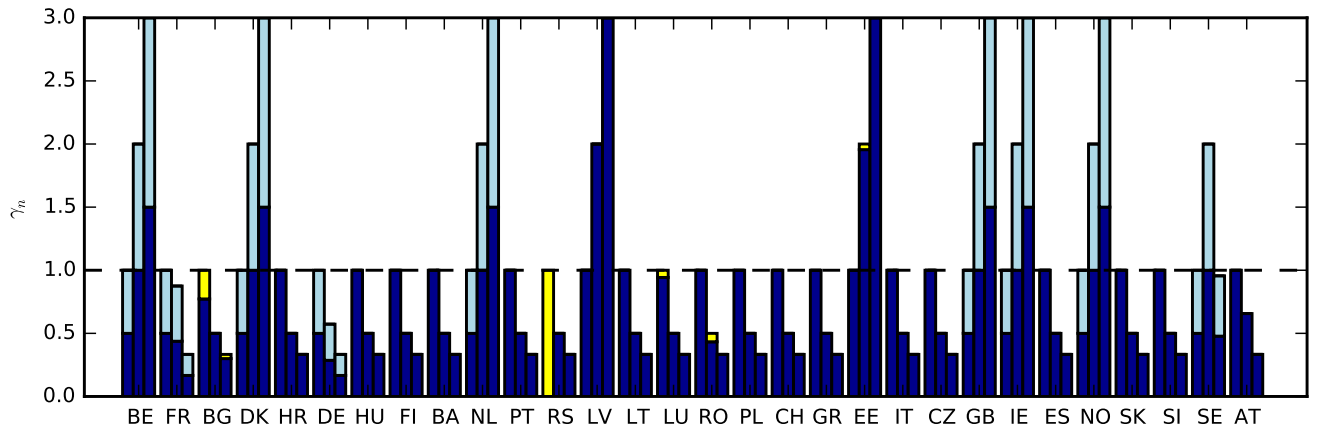

Figure 8: AGD layouts constrained by K = 1 (left), 2 (middle) and 3 (right) for an offshore share of 50% for Denmark, Germany, Great Britain, Ireland, the Netherlands, France, Belgium, Norway and Sweden.